Pharmaceutical Research, Vol. 25, No. 4, April 2008 (© 2007)
DOI: 10.1007/s11095-007-9411-4

Commentary

Projection of Exposure and Efficacious Dose Prior to First-in-Human Studies: How Successful Have We Been?

Christine Huang,[1,3] Ming Zheng,[2] Zheng Yang,[1] A. David Rodrigues,[1] and Punit Marathe[1]

Received April 2, 2007; accepted July 12, 2007; published online September 25, 2007

Purpose. Preclinical and clinical data for 35 proprietary Bristol-Myers Squibb discovery compounds (years 1997 to 2005) were collected and analyzed. In each case, exposure and efficacy in human subjects were projected at the time of nomination (for development) prior to first-in-human dosing.
Materials and Methods. Projections of area under the plasma concentration-time curve (AUC) in humans involved the use of one or more methods: (1) allometric scaling of animal pharmacokinetic data; (2) clearance projection employing *in vitro* data (liver microsomes and hepatocytes); (3) chimpanzee as an animal model; (4) the species-invariant time method; and (5) the Css-mean residence time or "Css-MRT" method. Whenever possible, prior clinical experience with lead compounds enabled the selection of the most appropriate method(s). Multiple approaches were also available at the time of the human efficacious dose projections: (1) efficacious exposure from animal efficacy models; (2) *in vitro* potency; and (3) prior experience with clinical leads.
Results. Over the 8 year period described, AUC in humans was projected within 2-fold (20 out of 35 compounds; 57%), greater than 2-fold to 4-fold (11 out of 35 compounds; 32%), and greater than 4-fold (4 out of 35 compounds; 11%) of the observed value. At the time of writing, clinical efficacy data were available for 10 compounds only. In this instance, the efficacious doses were also projected within 2-fold (7 out of 10 compounds; 70%), greater than 2-fold to 4-fold (2 out of 10 compounds; 20%), and greater than 4-fold (1 out of 10 compounds; 10%) of the actual clinical dose.
Conclusion. Overall, it was possible to project human exposure and efficacious dose within 4-fold of observed clinical values for about 90% of the compounds.

KEY WORDS: allometric scaling; efficacy; exposure; pharmacokinetics; projection.

INTRODUCTION

In recent years, the discovery and development of new medicines has become increasingly complex. For example, it is estimated that only about 10% of drug candidates that are selected for clinical development eventually become marketed drugs (1). This is largely because of novel targets with intricate underlying pharmacology, the desire for an optimal PK-ADME profile, increased focus on safety and risk-to-benefit considerations, and a more competitive marketplace. Projection of PK and efficacy prior to human dosing is a major effort during the characterization of lead compounds in discovery. The first-in-man dose selection is based on various pieces of information. Although no observable adverse effect level (NOAEL) is one of the important parameters that we typically use to guide dose selection, analysis of projection of human exposure and efficacious dose allows appropriate escalation of doses in the single ascending dose (SAD) studies to reach the efficacious dose–range quickly. Furthermore, human exposure and efficacious dose allow one to set safety margins (relative to animal toxicokinetic data), enables modeling of human PK at steady state, and focuses attention on the feasibility of various dosage forms and dosing regimens (e.g., twice-a-day *versus* once daily) at the time of nomination. In addition, the projection provides an early estimate of the amount of compound, which process chemistry needs to synthesize.

[1] Metabolism and Pharmacokinetics, Pharmaceutical Candidate Optimization, Bristol-Myers Squibb Co., P.O. Box 5400 Princeton, New Jersey 08543-5400, USA.
[2] Metabolism and Pharmacokinetics, Pharmaceutical Candidate Optimization, Wallingford, Connecticut 06492-7660, USA.
[3] To whom correspondence should be addressed. (e-mail: christine.huang@bms.com)

ABBREVIATIONS: ADME, absorption, distribution, metabolism, and excretion; AUC, area under the concentration *versus* time curve; AUC_{IPT}, area under the concentration *versus* time curve after intraportal administration; AUC_{IV}, area under the concentration *versus* time curve after intravenous administration; BMS, Bristol-Myers Squibb Co.; CL, clearance; CLhb, hepatic blood clearance; CLh,int, hepatic intrinsic clearance; C_{max}, maximum concentration; C_{min}, trough concentration; Css, dose divided by steady-state volume of distribution; E.R., hepatic extraction ratio; f_a, fraction of the dose absorbed; f_g, fraction of the dose escaping first-pass metabolism by the gastrointestinal mucosa; F_{PO}, oral bioavailability; f_u, fraction unbound; HH, human hepatocytes; HLM, human liver microsomes; IC_{50}, concentration required for 50% inhibition; IC_{90}, concentration required for 90% inhibition; IPT, intraportal; IV, intravenous; LC-MS/MS, liquid chromatography-tandem mass spectrometry; MRT, mean residence time; NOAEL, no observable adverse effect level; PB/PK, physiologically based pharmacokinetic model; PD, pharmacodynamics; PK, pharmacokinetics; Qhb, hepatic blood flow; Vss, steady-state volume of distribution.

Obviously, the projection of human PK involves the generation and integration of preclinical datasets, and numerous approaches have been published over the years (2–6).

When forecasting human PK prior to human dosing, special attention is paid to the AUC after oral dosing, elimination half-life, and peak-to-trough plasma concentration ratio. This is because adequate exposure (magnitude and duration) is required to ensure proof-of-concept (efficacy) in man. The projected elimination half-life provides an estimate of the frequency of drug administration in clinical studies. Frequently, adverse effects can be linked to the maximum concentrations in plasma (C_{max}) (7,8). Therefore, assessment of C_{max} is useful to avoid the unwanted toxicity often observed in animal species. At the same time, maintenance of adequate concentrations throughout the dosing interval is required for robust efficacy (9,10). This necessitates accurate assessment of trough concentrations (C_{min}) after a given dose. Developing and validating robust analytical assays with adequate sensitivity are important for the assessment. As described herein, there are at least five different methods that enable projections of human PK: (1) allometric scaling of animal PK data; (2) "scaling" of *in vitro* intrinsic clearance (liver microsomes and primary hepatocytes); (3) chimpanzee as an animal model; (4) the species-invariant time method; and (5) the Css-MRT method.

In terms of efficacy, a common approach is to study drug candidates in various animal species (e.g., mouse, rat, dog, rabbit, guinea pig, and monkey) and conduct detailed PD and PK (*versus* toxicological) characterization (11). Animal disease models are commonly used in many therapeutic areas, as part of target validation, which allows one to study drug behavior *in vivo*. In oncology, for example, nude mice transplanted with human xenografts are routinely used to assess the *in vivo* efficacy of anti-tumor agents (12,13). In immunology, rodents with arthritis, induced by agents such as collagen or adjuvant, are also common (14–16). Compounds acting on the central nervous system are evaluated similarly in various behavioral animal models, with a focus on brain penetration and target (e.g., receptor) occupancy (17,18). More recently, transgenic (humanized) animals have been described, which are particularly useful when pharmacological (target-related) species differences exist (19,20). Assessment of *in vivo* efficacy in these animal models, and integration with *in vitro* pharmacology data, is important when projecting human efficacious doses. However, antivirals are unique because animal models (e.g., human immunodeficiency virus and hepatitis C virus) are not readily available; therefore, it is common to move forward a compound directly into the clinic and evaluate viral load in patients (21–23). Nevertheless, it is still important to consider the target multiples of the *in vitro* IC_{50} (concentration required for 50% inhibition) or IC_{90} (concentration required for 90% inhibition), and relate them to the projected human PK profile.

At BMS, the importance of human PK and efficacious dose projections has been recognized. Unfortunately, the vast majority of literature reports have merely described retrospective analyses, wherein preclinical data have been correlated with existing clinical data for various drugs. No single report describing the prospective assessment of human PK and efficacious dose for a wide range of structurally diverse clinical candidates has been published. Therefore, the present discussion will focus on prospective assessment of 35 proprietary clinical candidates that span 8 years and 18 different therapeutic targets. The compound set includes 16 lead compounds (46%) and 19 back ups (54%). For each compound, preclinical and clinical data were collected and analyzed; both exposure and efficacy in human subjects were projected at the time of nomination prior to human dosing. Despite the limited clinical data, it was possible to evaluate the success of the efficacy projections for 10 of the compounds.

COMPOUNDS AND DATA SETS

Thirty-five proprietary discovery compounds were synthesized by the Department of Discovery Chemistry at BMS. These compounds belonged to various therapeutic areas and were nominated for clinical development between 1997 and 2005. A total of 16 lead compounds and 19 backups were included. Human PK information was available for each compound. In contrast, clinical efficacy data were only available for 10 of the compounds (29%).

In Vivo Preclinical Data. As part of lead characterization, *in vivo* PK studies were conducted in various animal species. These species included the mouse, rat, dog, cynomolgus monkey, and chimpanzee. Typically, animals received a single intravenous (IV) injection and single oral dose. The former involved a bolus or a short infusion. The oral dose was delivered by gavage as a solution, suspension, or capsule (filled with compound as solid powder or liquid). In each case, the choice of vehicles was dependent on the compound, therapeutic area, and animal species. Serial blood samples were collected, plasma prepared, and the samples processed appropriately. Concentrations of each compound in plasma were determined using valid liquid chromatography-tandem mass spectrometry (LC-MS/MS) assays. Plasma concentration *versus* time data were analyzed by noncompartmental methods using the KINETICA™ software program (Version 4.2 or equivalent version, InnaPhase Corporation, Philadelphia, PA) or a proprietary in-house mainframe software program known as PKMENU prior to year 2000. AUC was calculated using a combination of linear and log trapezoidal summations. The total plasma clearance and Vss were calculated after IV administration. The absolute bioavailability was estimated by taking the ratio of dose-normalized AUC value after the oral dose to that after the IV dose.

In vivo efficacy was assessed using various animal (e.g., mice, rats, rabbits, or guinea pigs) models representative of human diseases using a single or repeated oral dosing. Blood was sampled serially either from the same group of animals or a satellite group. Concentrations of each compound in plasma were determined using valid LC-MS/MS assays. In each case, systemic exposures (e.g., C_{max}, AUC, and C_{min}) required for efficacy or PD response were determined.

Clinical Data. PK information in humans (e.g., AUC) was obtained typically from the single ascending dose studies. The studies consisted of normal healthy volunteers or patients depending on the therapeutic area. Concentrations of each compound in plasma were determined using validated

LC-MS/MS assays. Exposure information was obtained at doses in the lower range of the dose-escalation scheme or from doses close to the projected efficacious doses. Proof of efficacious dose information in humans was obtained from either biomarker response in Phase I studies or doses selected for Phase II studies.

In Vitro Metabolism Data. For BMS compounds, turnover rate was calculated after incubation with liver microsomes or suspensions of primary hepatocytes; the rate was calculated based on disappearance of the parent compound by determining the nmoles of parent metabolized and dividing by the incubation time and the protein content. Intrinsic clearance was calculated by dividing the rate by the initial concentration in the incubation mixture. The *in vitro* intrinsic clearance was then scaled to an *in vivo* intrinsic clearance by using the appropriate scaling factors (5).

In Vitro Determination of Potency. In vitro potencies of the compounds, against the therapeutic target, were determined by optimized cellular assays and concentrations required for 50 or 90% inhibition (IC_{50} or IC_{90}) were calculated. The *in vitro* IC_{50} or IC_{90} values corrected for protein binding differences in the cell media (*versus* serum) were used to project efficacious doses in certain therapeutic areas.

HUMAN EXPOSURE PROJECTIONS

During the drug discovery stage, different methods are used to project human PK. Human exposure (AUC), which reflects the systemic exposure over the dosing interval and is a result of the entire ADME processes, was selected to assess the success of the projection. No attempt was made to correlate observed and projected peak-to-trough ratios in humans. The following methods have been successfully used for human exposure projections.

Allometric Scaling (Method 1). The concept of allometric scaling is based on the assumption that the anatomical, physiological, and biochemical variables of mammals can be scaled across species based on the body weight (24,25). The allometric approach is based on the power function, where the body weight of several species is plotted against the PK parameter of interest on a log–log scale as described in Eq. 1.

$$\text{Allometric Equation}: \log\ Y = \log\ a + b \cdot \log\ W \qquad (1)$$

where Y is a physiological parameter, log a is the y-intercept, b is the slope of the log–log plot, and W is the body weight.

The log–log plot of clearance (CL) *versus* body weight of the preclinical species then scales to human CL. Incorporation of allometrically scaled CL with oral bioavailability enabled projection of AUC in humans following an oral dose (Eq. 2).

$$\text{AUC} = \frac{F_{PO} \times \text{Dose}}{\text{CL}} \qquad (2)$$

For compounds with a low or intermediate hepatic extraction ratio (E.R.), the elimination is also dependent on biochemical parameters such as intrinsic clearance and protein binding. For some BMS compounds, protein binding and metabolic stability (microsomal or hepatocyte stability) correction factors have been applied to the allometric scaling. For example, protein binding (free fraction) was used as a correction factor for the clearance scaling for BMS-21. Protein binding (free fraction) and microsomal stability were used as correction factors for the clearance scaling for BMS-32. Correction factors were not applied for the rest of compounds.

Scaling of In Vitro Intrinsic Clearance (Method 2). Commonly used approaches for human PK projections rely on both *in vitro* and *in vivo* data from animal studies. Because the liver is the major clearance (metabolic) organ for most drugs, subcellular fractions such as hepatic microsomes and hepatocytes have been used to project *in vivo* hepatic clearance (3,25,26). Intrinsic clearance (CLh,int) and hepatic clearance were calculated based on the following equations.

The rate of oxidation in liver microsomes was determined as described in Eq. 3:

$$\text{Rate}(\text{nmol/min/mg protein}) = k \times C_0 / C_{\text{protein}} \qquad (3)$$

where k (min^{-1}) is the turnover rate constant estimated from the log–linear regression of the percentage of the compound remaining (y) *versus* time (t) curve using the following equation (Eq. 4)

$$y = y_{t=0} \times \exp(-kt) \qquad (4)$$

where C_0 (μM) is the initial drug concentration; and C_{protein} (mg/mL) is the microsomal protein concentration in the incubation.

Similarly, the rate of metabolism in hepatocytes was determined as described in Eq. 5:

$$\text{Rate}(\text{nmol/min/million cells}) = k \times C_0 / C_{\text{cell}} \qquad (5)$$

where C_0 (μM) is the initial drug concentration, C_{cell} (millions of cells/mL) is the hepatocyte concentration in the incubation, and k (min^{-1}) is the turnover rate constant estimated from the log–linear regression of the percentage of the compound remaining *versus* time curve.

The hepatic intrinsic clearance (CLh,int, mL/min/kg) in various species was estimated from liver microsome or hepatocyte data (25,27,28). Assuming linear kinetics, similar protein binding in microsomes (or hepatocytes) and blood, and similar CLh,int of unbound drug *in vitro* and *in vivo*, the CLh,int was calculated from the disappearance of the parent drug after incubating the drug with liver microsomes (Eq. 6) or hepatocytes (Eq. 7) as follows:

$$\text{Microsomes}: \text{CLh,int} = \left(\frac{k}{C_{\text{protein}}}\right) \times \left(\frac{45\ \text{mg protein}}{1\ \text{g liver weight}}\right) \times \left(\frac{\text{g of liver weight}}{\text{kg of body weight}}\right) \qquad (6)$$

$$\text{Hepatocytes}: \text{CLh,int} = \left(\frac{k}{C_{\text{cell}}}\right) \times \left(\frac{120 \times 10^6 \text{ cells}}{1 \text{ g liver weight}}\right) \times \left(\frac{\text{g of liver weight}}{\text{kg of body weight}}\right) \quad (7)$$

The liver weight relative to body weight in mice, rats, dogs, monkeys, and humans is 88, 40, 32, 32, and 21 g/kg, respectively (29). Assuming the well-stirred model of hepatic clearance, the hepatic blood clearance (CLhb, mL/min/kg) was estimated without correction for binding to blood or microsomal proteins as described (Eq. 8):

$$\text{CLhb} = \frac{\text{Qhb} \times \text{CLh,int}}{\text{Qhb} + \text{CLh,int}} \quad (8)$$

where Qhb is the hepatic blood flow with a value equals to 90, 55, 31, 40, and 21 mL/min/kg in mice, rats, dogs, monkeys, and humans, respectively (29).

At times, based on the scientist's understanding of the molecular descriptors (e.g., lipophilicity, acidity) and physiologic behavior of BMS compounds, CLhb was projected with correction for plasma protein binding as described in Eq. 9.

$$\text{CLhb} = \frac{\text{Qhb} \times f_u \times \text{CLh,int}}{\text{Qhb} + f_u \times \text{CLh,int}} \quad (9)$$

The projected hepatic clearance was compared to the observed *in vivo* clearance in each animal species evaluated. If the two values were in reasonable agreement (e.g., within 3-fold), systemic clearance in humans was projected from the corresponding *in vitro* human system. If a correction factor could be identified for projection of *in vivo* clearance across all the animal species evaluated, a similar correction factor was employed to project human *in vivo* clearance (25).

In addition, based on the hepatic clearance either projected from *in vitro* data or observed in animals, as well as animal oral bioavailability, the fraction of dose absorbed into the portal vein ($f_a \times f_g$) can be estimated, which in turn can be used to project human oral bioavailability by considering first-pass liver metabolism estimated from *in vitro* human data. The fraction of dose absorbed into the portal vein in animal species is estimated as described in Eq. 10:

$$f_a \times f_g = \frac{F_{\text{po,animal}}}{\left(1 - \frac{\text{CLhb,animal}}{\text{Qhb,animal}}\right)} \quad (10)$$

The average value of ($f_a \times f_g$) from animal species is then used along with human *in vitro* data from either liver microsomes or hepatocytes to project human oral bioavailability (Eq. 11):

$$F_{\text{po,human}} = (f_a \times f_g) \times \left(1 - \frac{\text{CLhb,human}}{\text{Qhb,human}}\right) \quad (11)$$

The estimated $F_{\text{po, human}}$ was then used to calculate human AUC based on the Eq. 2.

Use of Chimpanzee as an Animal Model (Method 3). Other than typical laboratory animals (i.e., mouse, rat, dog, and cynomolgus monkey), the chimpanzee (*pan troglodytes*) has been used occasionally for projection of human PK. The chimpanzee has 98.8% genetic similarity to human (30). Furthermore, the chimpanzee has similar anatomy, physiology, and endocrinology compared to human and has been used for safety, human disease, and PK assessment by some investigators (31–33). Although Qhb is comparable (chimpanzee *versus* human), chimpanzee hepatic microsomal cytochrome P450 activities are not fully characterized and species differences are possible. Therefore, its use for human PK projection should be examined carefully. When the metabolism of BMS proprietary compounds was determined to be cytochrome P450 dependent, and turnover rates were similar in liver microsomes (chimpanzee *versus* human), the chimpanzee was used to project human AUC. The human AUC was calculated from the chimpanzee AUC, assuming a one-to-one correspondence.

Species-Invariant Time Method (Method 4). Dedrick plots and related modified methods are based on the concept of physiological time, with the concentration-time profile in animals being transformed by correction factors to yield a human profile (24,34). The species-invariant time method is based on the theory that a complex Dedrick plot, with exponents obtained from best fitting of the animal intravenous plasma concentration-time profiles, can generate a human plasma concentration-time profile by correlating variations in biological structure (e.g., blood vessel size) and metabolic rates (e.g., glomerular filtration rate) (34,35). The dose normalized plasma concentrations and time data from preclinical species (e.g., rat, dog, and monkey) were transformed by dividing the dose normalized concentrations (Y axis) and time (X axis) by the body weight to a power. The best fit of the exponents of body weight was used to transform and project the plasma concentration *versus* time profile in man (Eq. 12).

$$\frac{C}{\left(\frac{\text{Dose}}{\text{Body Weight}^Y}\right)} = A \times \exp\left(\frac{-\alpha \times t}{\text{Body Weight}^X}\right) + B \times \exp\left(\frac{-\beta \times t}{\text{Body Weight}^X}\right) \quad (12)$$

After IV and oral dosing in animals, and deconvolution of the plasma concentration-time data, the parameters related to oral absorption (i.e., absorption rate constants and extent of absorption) were obtained using the KINETICA™ software. The oral absorption parameters were either averaged across species, or were based on the experience with a previous clinical candidate (e.g., dog or monkey was taken as a representative of oral absorption in humans). These parameters along with the predicted IV PK profile were used to project AUC in humans following an oral dose.

Css-MRT Method (Method 5). Another method employed to project plasma concentration-time profiles was taken from Wajima et al. (36). This method is based on the assumption that concentration-time profiles are linear and similar across species including humans, and that normalized curves derived from a variety of animal species can be superimposed. The normalized curve is derived by dividing the concentration and time scales by Css (defined as dose/Vss) and MRT, respectively (Eq. 13). It is assumed that the

AUC in humans can be obtained by multiplying the concentration and time scales of the normalized curve obtained from the animal data by projected Css and MRT in humans, respectively.

$$\frac{C}{\text{Css}} = A \times \exp\left(\frac{-\alpha \times t}{\text{MRT}}\right) + B \times \exp\left(\frac{-\beta \times t}{\text{MRT}}\right) \quad (13)$$

Experience with Clinical Leads (Method 6). In some therapeutic areas, human PK data were available for compounds already in clinical development. Therefore, for these compounds at the time of nomination, it was possible to project human exposure based on methods similar to those used for the lead compound and by applying the appropriate correction factors. For example, the correction factor can be the ratio of animal species AUC vs. human AUC for the lead compound. However, the application of a correction factor highly depends on the therapeutic area and compound. Only when the backup and lead belong to the same chemotype and have similar ADME properties, the same projection method(s) can be used for the backup compound.

PROJECTIONS OF EFFICACIOUS DOSE

Exposure Required for Efficacy in Animal Disease Models (Method 1). Animal models have been widely used in various therapeutic areas to mimic human diseases. Such models are useful and enable PK/PD modeling approaches. By combining the projected PK parameters, plasma concentration-time profile using the methods described above, and the exposure required for efficacy in animal disease models, it was possible to project efficacious dose in humans. For example, if a minimum AUC is necessary for demonstrating efficacy in the animal model, that AUC along with projected human CL and oral bioavailability were used to project human efficacious dose (Eq. 2). When the chimpanzee PK profile was used to project human PK, the PK profile in chimpanzees was combined with the efficacy data in animal disease models to project the human efficacious dose. A correction for species differences in potency against the target was applied whenever necessary.

A specialized approach was adopted to estimate human efficacious dose and exposure when the liver was the target organ. The compound was administered via IV, intraportal (IPT), and oral routes to rats and guinea pigs and liver exposure, oral absorption, and hepatic extraction ratio were determined. Hepatic extraction was calculated according to the Eq. 14:

$$\%\ \text{hepatic extraction} = 1 - (\text{AUC}_{\text{IPT}}/\text{AUC}_{\text{IV}}) \quad (14)$$

where AUC_{IPT} and AUC_{IV} are the areas under the curve after IPT and IV administration, respectively. The absolute oral bioavailability (expressed as %) was estimated by taking the ratio of the dose-normalized AUC value after an oral dose to that after an intravenous dose. Liver exposure was calculated as the maximum amount of the compound available in liver (dose $\times f_a \times$ E.R.). Oral exposure (and bioavailability) alone did not accurately project the efficacy of the compound, and in some instances liver exposure was thought to more accurately reflect how much compound was needed for efficacy.

Exposure Required to Maintain Adequate In Vivo Concentrations Based on In Vitro Potency (Method 2). In many disease areas (e.g., antiviral, ion channel inhibition, oncology, and thrombosis), a good correlation has been demonstrated between *in vitro* potency and *in vivo* activity (37). For example, free plasma concentrations and the *in vitro* IC_{50} value for potassium channel blockade are used for projection of concentrations at which QT prolongation may be a safety risk. In certain therapeutic areas, an *in vivo* animal disease model representative of human disease is not available (38,39). In such cases, it is necessary to project human efficacious dose by considering *in vitro* potency as a threshold effect (i.e., IC_{50} or IC_{90}) in relation to the projected human PK (AUC) profile. Human exposure projection method 4 or 5 was used to project human PK profile for maintaining required C_{min} for efficacy. When deemed important, potency was adjusted by protein binding. For example, in the antiviral therapeutic area, reasonable relationships have been shown between maintenance of C_{min} at IC_{50} or IC_{90} against the target and reduction in viral load (40,41).

Experience with Clinical Leads (Method 3). Prior experience garnered with drugs already in clinical trials, which have shown proof of concept, can provide significant insight into the PD of the new chemical entity in question. The feedback from such clinical leads is extremely important because back-up compounds are often from a similar chemotype or have similar physicochemical properties and mechanism of action. Therefore, lead compounds can be used to set up correction factors that can be applied when projecting efficacious dose.

ASSESSMENT OF PROJECTIONS

To assess the success of the projections, the projected AUC value (and efficacious dose) was compared to the observed clinical data. When two AUC (and efficacious dose) values were projected an arithmetic mean was calculated and used for the assessment. When the "projection ratio" (observed *versus* projected, observed/projected; or projected *versus* observed, projected/observed) was within 2-fold, the projection was considered "accurate." A projection ratio of greater than 2-fold and up to 4-fold was characterized as "acceptable." A projection ratio of greater than 4-fold indicated that an improvement was needed and likely reasons for the discrepancy were investigated. The success (bias) of the projections was assessed by calculation of the geometric mean of the ratio of projected and observed values (average fold error) for all compounds in the dataset (Eq. 15) (5,42).

$$\text{Average fold error} = 10^{\left[\frac{\sum \left|\log \frac{\text{Projected}}{\text{Observed}}\right|}{N}\right]} \quad (15)$$

Table I. Human Exposure (AUC) Projection Summary

Year	Compound	Dose	Projected AUC	Observed AUC	Projection Ratio[a]	Methodology	Observed Variability
AUC (μM × h) projection ratio ≤2							
1997	BMS-1	65 mg/m^2	3.8	5.1	1.3	Method 1	CV 35%
1997	BMS-2	60 mg/m^2	2.4	3.1	1.3	Method 1	CV 27%
1998	BMS-3	50 mg/m^2	2.8	5.3	1.9	Method 1	Range 2.4–10.7
1999	BMS-4	50 mg/m^2	3.4	5.7	1.7	Method 1	CV 47%
1999	BMS-5	250 mg	21.5, 8.7 (15)[c]	25.4	1.7	Method 1, Method 2	Range 14.2–35.5
2000	BMS-6	10 mg	0.7	0.5	1.4[b]	Method 1	Range 0.26–0.59
2000	BMS-7	47 mg/m^2	7.6	5.5	1.4[b]	Method 1	CV 40%
2001	BMS-8	200 mg	23.7	28.4	1.2	Method 2	CV 21%
2001	BMS-9	100 mg	6.0	4.4	1.4[b]	Method 1	Range 3.2–6.7
2001	BMS-10	150 mg	0.28, 1.9 (1.1)[c]	0.81	1.3[b]	Method 6—mouse, Method 6—dog	Range 0.3–1.75
2002	BMS-11	100 mg	23	25	1.1	Method 3	CV 15%
2002	BMS-12	600 mg	138, 539 (339)[c]	193	1.8[b]	Method 6—dog, Method 6—monkey	CV 15%–27%
2002	BMS-13	100 mg	1.6, 0.27 (0.9)[c]	0.72	1.3[b]	Method 2—HH, Method 2—HLM	Range 0.17–1.34
2002	BMS-14	20 mg	3.1	2.4	1.3[b]	Method 4 and 6	CV 23%
2003	BMS-15	100 mg	11.4	13.3	1.2	Method 6	10.3–15.6
2003	BMS-16	600 mg	91, 42 (67)[c]	87	1.3	Method 2—HLM, Method 2—HH	Range 61.8–118
2003	BMS-17	5 mg	1.0	1.3	1.3	Method 3	CV 15%
2004	BMS-18	50 mg	11.3, 7.1 (9.2)[c]	10.7	1.2	Method 4, Method 5	CV 18%
2004	BMS-19	800 mg	116	156	1.3	Method 2—HH	CV 13%
2005	BMS-20	20 mg	5.7, 8.3 (7.0)[c]	9.7	1.4	Method 4, Method 5	CV 13%
AUC (μM × h) projection ratio >2 to 4							
1999	BMS-21	200 mg	120	33.5	3.6[b]	Method 1	CV 18%
2000	BMS-22	100 mg	1.0	0.3	3.3[b]	Method 2	CV 23%
2002	BMS-23	320 mg	11.8	30.1	2.6	Method 1	Range 23–48
2002	BMS-24	10 mg	10	3	3.3[b]	Method 3	Range 1.8–4.4
2003	BMS-25	100 mg	3.2	9.3	2.9	Method 1, Method 2	Range 2.6–13.5
2003	BMS-26	20 mg	0.04	0.09	2.4	Method 6—rat PK	Range 0.05–0.13
			0.4			Method 6—guinea pig PK	
2003	BMS-27	50 mg sol	0.75	3.7	4.9	Method 3	Range 2.3–4.7
		200 mg cap	3.0	0.89	3.4[b]		Range 0.68–1.6
		400 mg cap	6.0	3.2	1.9[b]		Range 2.4–5.7
2004	BMS-28	2.5 mg	5.8	1.7	3.4[b]	Method 3	CV 29%
2004	BMS-29	25 mg	17.5	5.0	3.5[b]	Method 6	Range 3–9
2004	BMS-30	10 mg	448, 714 (581)[c]	201	2.9	Method 2—HH	Range 98–225
2005	BMS-31	30 mg	814	2,084	2.6	Method 1	Range 1,362–2,862

AUC (μM × h) projection ratio >4						CV>70%
2001	BMS-32	3 mg	0.03	0.006	5[b]	Method 1	CV 28%
2001	BMS-33	100 mg	0.3	11	37	Method 3	Range 50.4–120
2002	BMS-34	300 mg	6.6	82.9	13	Method 1	CV 19%
2003	BMS-35	20 mg sol	1.9	3.2	1.7	Method 3	CV 34%
		200 mg cap	19	4.4	4.3[b]		

HLM Human liver microsomes; *HH* human hepatocytes; *CV* coefficient of variation
[a] Unless otherwise indicated, data are reported as the ratio of observed *versus* projected AUC (observed AUC/projected AUC).
[b] Observed AUC < projected AUC and the ratio is reported as projected *versus* observed AUC (projected AUC/observed AUC).
[c] Mean value of projected AUC values

RESULTS

AUC Projections. Data for all 35 compounds are shown in Table I. In the table, the year of nomination and the clinical dose at which the actual human exposure (AUC) was obtained are shown. The observed AUC is a mean of the AUC values from a group of healthy normal volunteers or patients. Variability (inter-subject) associated with the observed AUC is also included in the table. The variability is either expressed as the coefficient of variation of mean AUC values or the range of AUC values at the dose administered. The methodology used in the projection of human AUC is also shown. For many of the compounds (~50%), allometric scaling or scaling *in vitro* clearance was employed.

As summarized in Table II, it was possible to project successfully the human AUC (projection ratio ≤2) for 20 out of 35 compounds (57%). For 11 out of 35 compounds (32%), projections of human AUC fell >2-fold to 4-fold of the observed value. For the remaining compounds (4 out of 35 compounds; 11%), the projection ratio was >4. The geometric mean of the ratio of projected and actual values for all compounds in the dataset (average fold error) was 2.17. Figure 1 shows the projected *vs*. observed AUC values for all the compounds in the dataset and compounds characterized by a ratio of greater than 4 are indicated. The likely reasons for the discrepancy between the observed and projected values are briefly discussed below.

AUC Projection Ratio ≤2. BMS-1, BMS-2, BMS-3, BMS-4, and BMS-7 are anticancer compounds intended for IV dosing. Human clearance for these compounds was projected based on simple allometric scaling. Observed human exposure in all cases was within 2-fold of the projected value. The success of these projections was largely due to the fact that no additional factors, such as differences in formulation and oral bioavailability, in various animal species needed to be considered.

For some compounds shown in Table I, two values for human AUC were projected. These values are a result of the different methodologies used. For BMS-5, allometric scaling of oral clearance yielded a value of 5.4 mL/min/kg with a projected AUC of 21.5 μM×h at a dose of 250 mg. A second approach yielded a projected AUC of 8.7 μM×h at a dose of 250 mg and was based on hepatic clearance projected from human hepatocytes (8 mL/min/kg) and the calculated fraction extracted by the liver during first pass (assuming fraction absorbed and fraction escaping through the gut as unity). The observed AUC of 25.4 μM×h resembled the projected AUC from the allometric scaling of oral clearance. At higher doses (data not shown); however, the observed AUC values were closer to that projected from human hepatocytes. This is probably due to solubility-limited absorption of BMS-5, rather than matching clearance values from the hepatocyte data.

For some compounds, significant species differences in PK were observed and a range of projected values was shown. For BMS-12, the absolute oral bioavailability in the dog and monkey was 40% and ~100%, respectively. Based on the body surface area conversion from these two non-rodent species (43) and assuming the oral bioavailability will be similar in humans, a range of AUC values of 138 μM×h (dog) to 539 μM×h (monkey) was projected at a dose of 600 mg. The conversion number to convert animal dose in mg/kg to human equivalent dose in mg/kg was 1.8 and 3.1 for dogs and monkeys,

Table II. Overall Success Rate for the Projection of Human Exposure and Efficacious Dose

Assessment of the Projection (Projection Ratio)[b]		Human Exposure (AUC) (35 compounds)	Human Efficacious Dose (10 compounds)
Accurate	≤2	20 (57%)[a]	7 (70%)
Acceptable	>2 to 4	11 (32%)	2 (20%)
Needs Improvement	>4	4 (11%)	1 (10%)

[a] Values in parentheses represent percent of total number of compounds in the dataset.
[b] For both AUC and efficacious dose, the projection ratio is defined as the ratio of observed *versus* projected (observed/projected) or projected *versus* observed (projected/observed).

respectively. The calculated AUC value at 600 mg (based on actual data at 400 and 800 mg data) was 193 μM×h and was bracketed by the projections based on the dog and monkey. The oral bioavailability of BMS-12 in humans may be similar to the value in dogs. A similar situation was observed with BMS-10. In this instance, allometric scaling was used to project human clearance. However, species differences in the oral bioavailability (mouse, 6%; and dog, 40%) led to a range of projected AUC values (0.28 to 1.9 μM×h at a dose of 150 mg). The observed AUC value following a 150 mg dose was 0.81 μM×h.

When the administered compound is a prodrug, projection of human exposure from preclinical species is quite challenging. BMS-12, BMS-16, and BMS-19 are examples of such prodrugs. BMS-12 is a dioxolane prodrug, BMS-16 is an alanine ester prodrug, while BMS-19 is a phosphate prodrug, synthesized to increase either the permeability or aqueous solubility of the parent compound. The PK and oral bioavailability of these prodrugs were assessed in preclinical species, and *in vitro* in animal and human gut and liver subcellular fractions, in order to ensure conversion of the prodrugs to the active moiety. In all cases, rapid and complete conversion of the prodrugs to the active moieties was used in the projection of the human exposure and efficacious doses.

Some discovery programs used both HLM and human hepatocytes for projection of human clearance. BMS-13 belonged to such a program. In this case, the turnover of BMS-13 was faster in HLM compared to human hepatocytes and the projected human clearance was 17 and 10 mL/min/kg, respectively. Incorporation of hepatic extraction, calculated from projected clearance, led to the projected AUC value of 0.27 μM×h (HLM) and 1.6 μM×h (human hepatocytes) at a dose of 100 mg. For BMS-16, turnover in HLM was slower compared to human hepatocytes and the projected AUC values were 91 and 42 μM×h, respectively, at a dose of 600 mg after consideration of oral absorption and hepatic extraction. The observed AUC values for BMS-13 and BMS-16 were covered by the range of projected AUC values (Table I).

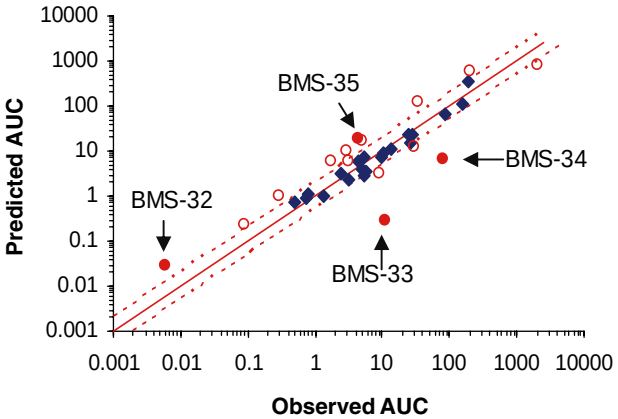

Fig. 1. Plot of observed AUC values *versus* projected AUC values. *Solid line* represents the line of identity. *Dashed lines* represent a 2-fold error. *Filled diamonds*, compounds with projection ratio ≤2. *Open circles*, compounds with projection ratio >2 to 4. *Filled circles*, compounds with projection ratio >4

Both the species-invariant time method and Css-MRT method were employed for projection of human exposure of BMS-18 and BMS-20. For BMS-18, the former yielded a value of 11.3 μM×h while the latter yielded a value of 7.1 μM×h at a dose of 50 mg. The observed mean AUC value was 10.7 μM×h at the same dose. For BMS-20, the projected AUC values using the species-invariant time and Css-MRT methods were 5.7 and 8.3 μM×h, respectively, compared to the observed AUC (9.7 μM×h) at 20 mg.

Experience with lead compounds was important for the AUC projection of BMS-14 and BMS-20. In both cases, the exposure projections for the backup compounds were closer to the actual values compared to those for the lead compounds. BMS-14 was the backup for BMS-21. Both the compounds belonged to the same chemotype and exhibited similar ADME properties. Exposure of BMS-21 in man was 3.6-fold lower than the projected value, although it was noted that the human PK profile was similar to that of the dog. Because the profile of BMS-14 was similar to BMS-21 in the dog, the AUC of BMS-14 in man was projected to be similar to that of BMS-21. In agreement, the projected and observed AUC of BMS-14 was 3.1 and 2.4 μM×h, respectively. BMS-20 was the backup to BMS-12 and a retrospective projection of human AUC for the latter, using the Css-MRT method, yielded a value of 167 μM×h (*versus* an observed AUC of 193 μM×h). The original prospective projection was 138 and 539 μM×h based on dog and monkey PK, respectively. As a result, the same approach (Css-MRT method) was applied for the projection of BMS-20; the projected human AUC was 1.4-fold of the observed AUC.

AUC Projection Ratio >2 to 4. BMS-23 is the lead of BMS-30. Method 1 (allometric scaling) provided 3-fold lower projection of AUC in man for BMS-23. When Method 2 (scaling of *in vitro* intrinsic clearance) was used for BMS-30, it generated a projection with a comparable fold-error (3-fold higher compared to the observed AUC). The benefit of the clinical experience was not used for the human AUC projection for BMS-30 because these compounds are classified as different chemotypes and eliminated through different metabolic pathways.

Method 1 and 2 were used to project human AUC for BMS-25 (clinical lead), while only method 1 was use for BMS-31 (back-up compound). Method 2 was not used for BMS-31 because there was no turn over in microsomal and hepatocyte stability studies.

BMS-26 required a specialized approach with liver as the target organ. For this compound, the extent of oral absorption and hepatic extraction in rats were 20 and 86%, respectively, while in guinea pigs oral absorption was 64% and hepatic extraction was 35%. However, liver exposure to BMS-26 was similar in both rats and guinea pigs. The projected human efficacious dose was then estimated to be 19 and 14 mg based on the liver exposure required for efficacy in the two species, respectively. After incorporation of the oral bioavailability values obtained from these two preclinical species and systemic clearance obtained from allometric scaling, the projected human AUC associated with the projected efficacious dose was calculated to be 0.04 μM×h (based on the rat PK) and 0.4 μM×h (based on the guinea pig PK). The mean observed AUC in humans was 0.09 μM×h (range=0.05–0.13 μM×h) at a dose of 17 mg, within 4-fold of the projection.

The chimpanzee was used for human AUC projections for two programs with projected human AUC within 4-fold of the observed AUC. BMS-28 was the backup for BMS-24. The projected human AUC was 3.3- and 3.4-fold of the observed AUC for BMS-24 and BMS-28, respectively. Likewise, the chimpanzee PK was used for the human AUC projection for BMS-27. BMS-27 was the backup for BMS-22. Because the chimpanzee PK of BMS-22 showed similar rapid oral absorption and fast decline of plasma concentration after T_{max}, chimpanzee PK was used for projecting human AUC for BMS-27. The projected human AUC at 200 mg was within 4-fold of the observed AUC. However, because of the low aqueous solubility of BMS-27, the observed human AUC decreased significantly when BMS-27 was dosed in a capsule (3.7 μM×h for 50 mg in solution *versus* 0.89 μM×h for 200 mg in capsule).

AUC Projection Ratio >4. As shown in Table I, only 4 out of 35 compounds (11%) were problematic. Exposure to BMS-32 and BMS-35 in man was over-projected. These are compounds with very low aqueous solubility (<0.01 mg/ml). In preclinical studies, it was found that the oral absorption of these compounds was dissolution-rate limited and as such, formulation plays a vital role in determining exposure after oral administration. During lead characterization, preclinical studies of BMS-32 were carried out using a vehicle containing a large proportion (67%) of non-aqueous solvents and the average oral bioavailability was determined to be 25%. After nomination of BMS-32 for development, further optimization of the form and formulation was undertaken for clinical use. Preclinical studies were repeated to assess oral exposure for BMS-32 using the final form and formulation selected for development. The oral bioavailability was determined to be around 10% in preclinical species. Retrospective calculation of human exposures based on the 10% oral bioavailability would have led to a projection within 2-fold of the actual exposure. For BMS-35, the projected exposure was 1.9 μM×h at a low dose (20 mg) which was within 2-fold of the observed exposure (3.2 μM×h). However, because of the dissolution rate-limited absorption, the observed exposure at the high dose (200 mg) was lower than 4-fold of the projected value.

Human exposure of BMS-33 was projected based on the exposure observed in chimpanzees, and one possible reason for the under-projection of the human AUC is species differences in metabolism (humans *versus* chimpanzees). However, a more likely explanation is the limited formulation options available for PK evaluation in the chimpanzee at the time of nomination. Therefore, the vehicles used in the chimpanzee studies were not optimal for maximizing oral exposure and may have resulted in under-projection of human exposure.

Human exposure for BMS-34 was under-projected by allometric scaling. Applying the elementary Dedrick plot method, the human plasma concentration-time profile of BMS-34 was retrospectively compared to that of animals. The results revealed that the human profile best resembled the dog concentration-time profile. Subsequently, the same approach was used to prospectively project the human plasma concentration-time profile of the backup compound (BMS-29), resulting in a significant improvement in the projection of human AUC and concentration-time profiles (3.5-fold of the actual clinical exposure).

Table III. Human Efficacious Dose Projection Summary

Year	Compound	Projected Dose	Observed Dose	Projection Ratio[a]	Methodology
Efficacious dose projection ratio ≤2					
2002	BMS-24	4–13 mg (8.5 mg)	10 mg	1.2	Method 2
2002	BMS-12	900 mg BID	1,200 mg BID	1.3	Method 2
2003	BMS-27	205 mg	400 mg	2.0	Method 2
2002	BMS-13	33–176 mg (105 mg)	50–150 mg (100 mg)	1.0	Method 1
2002	BMS-23	500 mg	500–600 mg (550 mg)	1.1	Method 3
2003	BMS-16	570–1,300 mg (935 mg)	320–600 mg (460 mg)	2.0[b]	Method 1
2003	BMS-26	17 mg	20 mg	1.2	Method 3
Efficacious dose projection ratio >2 to 4					
2002	BMS-34	300 mg	400–1,000 mg (700 mg)	2.3	Method 2
2003	BMS-25	70 mg	30 mg	2.3[b]	Method 1
Efficacious dose projection ratio >4					
1998	BMS-36	150 mg	25 mg	6[b]	Method 2

[a] Unless otherwise indicated, data are reported as the ratio of observed *versus* projected dose (observed dose/projected dose).
[b] Observed dose < projected dose and the ratio is reported as projected *versus* observed dose (projected dose/observed dose).

Table IV. Impact of Projection Range on Human Dose and Exposure Projection

Projection Range	Human Exposure (AUC) (35 compounds)	Human Efficacious Dose (10 compounds)
Single value	26 (73%)[a]	7 (70%)
<2-fold	3 (9%)	0 (0%)
2- to 4-fold	3 (9%)	2 (20%)
>4- to 10-fold	3 (9%)	1 (10%)

[a] Values in parentheses represent percent of total number of compounds in the dataset.

Efficacious Dose Projections. The human efficacious dose projections are shown in Table III. Observed efficacious doses were obtained from phase II efficacy studies or from biomarker endpoints obtained in phase I studies. For 3 out of 10 compounds, a range of efficacious doses is projected. For BMS-13 and BMS-16, the range of doses is simply a reflection of the range of projected human exposures as described earlier. For BMS-24, the range is based on the two different efficacy models in the rabbit and the need to maintain plasma concentrations at the end of the dosing interval.

For 7 out of 10 compounds, it was possible to project successfully the human efficacious dose within 2-fold of the observed dose. For 2 out of 10 compounds (BMS-25 and BMS-34), a reasonable projection of the human efficacious dose was obtained (projection ratio=2.3). The human efficacious dose projection ratio for one compound (BMS-36) was >4 (Table II).

Whenever possible, attempts were made to use the experience gained with lead compounds. For example, BMS-23 is targeted for cancer treatment and the efficacious human dose based on efficacious exposures in the mouse xenograft models would have been 2,000 mg. However, experience with a competitor compound in the clinic revealed that the efficacious exposure in the mouse was 6.5-fold higher than that required in clinical trials. The projected human dose was thus refined to 500 mg with this adjustment and after consideration of differences in serum protein binding (mouse *versus* human).

For BMS-34, the AUC was under-projected by >4-fold, although the projected dose was 2.3-fold based on biomarker data. This shows that perhaps the biomarker response is not directly related to the plasma AUC. However, a comparable corollary was observed with BMS-25 where the observed exposure was >2-fold to 4-fold greater than projected value and the observed efficacious dose was >2-fold to 4-fold less than projected value. For BMS-36, there was no prospective projection of human AUC since the dose was projected based on the maintenance of adequate trough concentrations.

Projection Ranges. Table IV categorizes the compounds on the basis of the projection range, and for 26 out of 35 compounds a single value was projected for human AUC. For 9 out of 35 compounds, a range of AUC values was projected, with only 3 compounds having an AUC projection range of greater than 4-fold. Similarly, only 1 out of 10 efficacious dose projections was reported as a range (>4-fold). Therefore, the success of the projections was not based on a wide range of projected AUC or efficacious doses.

DISCUSSION

As described herein, 35 proprietary compounds were nominated over an eight year period and, indeed, it was possible to project human AUC and efficacious dose within 4-fold of the observed value for about 90% of them. For the sake of brevity, the following discussion will focus on key points.

Linearity of PK. An important assumption throughout the various projections was that each compound exhibited linear PK in animals and man. Linearity was also assumed when projections were based on scaled *in vitro* intrinsic clearance. In order to compare the PK under linear conditions, the dose used for human AUC projection was chosen from the low end of the single ascending dose studies. The very first dose used in first-in-human studies was generally avoided since at this dose, characterization of the complete plasma concentration-time profile was difficult because of the limited sensitivity of the bioanalytical methods. As the dose level increases, a compound may exhibit non-linear PK because of saturation of metabolic and/or transporter pathways involved in disposition. At higher doses, drugs can often demonstrate flip-flop or absorption limited kinetics, which invalidates the assumptions underpinning the projections. Furthermore, plasma exposure may decrease due to dissolution rate or solubility-limited absorption.

Another important point is that all the AUC projections described were based on observations after a single dose. When a linear PK profile prevails, the area under the plasma concentration-time curve from zero to infinity (AUC(INF)) is the same as the area under the plasma concentration-time curve over a dosing interval at steady state (AUC(TAU)). However, if the steady state human PK cannot be projected based on the single dose data, it is difficult to project steady state human AUC based on preclinical data. This leads to erroneous projections of efficacy, especially when chronic dosing is required.

Species Differences in Clearance and Metabolism. Although animal PK data are useful, there is no general agreement as to which species best represents human. The literature provides examples of a number of empirical approaches when such analyses are carried out retrospectively, e.g., use of the rat for bioavailability and Vss (2), and use of the monkey for fraction of dose absorbed (44). However, it is difficult to assess the correlation of human and preclinical species when attempting to "prospectively" project clinical outcomes. In our experience, occasionally it was possible to consider the similarity in the *in vitro* metabolic profile as a determinant of which species may (or may not) be more predictive of human. If a compound showed a propensity for Phase II metabolism (e.g., direct glucuronidation or sulfation), then primary hepatocytes were employed as much as possible (45,46). Unique metabolic pathways in man, enterohepatic circulation, and species differences in the conversion of prodrugs to the active moiety, were additional complicating factors that had to be considered routinely.

Despite concerns related to species differences, several correction factors such as maximum life span potential and brain weight have been proposed for the projection of human clearance (47). For compounds eliminated through metabolism, metabolic turnover from *in vitro* liver microsomes or hepatocyte incubations has been used to improve human clearance projections (48). However, there is evidence that wholesale application of these correction factors has not substantially improved the accuracy of such projections (49). Notably, the compounds described herein belong to different chemotypes and are characterized by different PK/ADME profiles. Therefore, instead of applying a uniform approach, or a correction factor, the unique properties of each compound (across species) were considered as much as possible at the time of nomination.

Optimization of Formulation. Very often in drug discovery, preclinical PK studies are conducted with less than the most optimal form of the drug substance. These studies are also often conducted by administering the compound(s) in a mixture of non-aqueous solvents. The former situation is likely to reduce the observed exposure while the latter is likely to increase the exposure observed in preclinical species. These uncertainties need to be considered when anticipating oral bioavailability in humans. For example, oral exposure for a compound with dissolution-rate limited absorption is likely to decrease from a solid dosage form. Unfortunately, most formulation efforts only start after the compound is nominated for development. Such efforts lead to selection of the most optimal form (salt, free base, or specific polymorph) and enable optimization of formulations after selection of the most appropriate excipients. The selection of the best form and formulation at the development stage is likely to yield oral exposures at least similar to, or at times greater than, those obtained in a discovery setting.

The concept of maximum absorbable dose is used in the pharmaceutical industry to ascertain the feasibility of delivering the amount of dose needed for pharmacological activity (4,50). While this number is obtained based on the solubility and permeability of the drug molecule, one can only use it as a guide. Often, the solubility of the drug molecule in the gastrointestinal tract exceeds the solubility measured in the dissolution medium by many fold and as such, the projected maximum absorbable dose is likely to be many fold lower than the actual dose that can be delivered (4,51–53).

Projection of PK Profiles. Although the present discussion is focused on the projection of AUC, it is important to note that projections of the overall plasma concentration-time profile (e.g., C_{max}, C_{min}, or half-life) are also valued indicators. Many biological targets require maintenance of plasma concentrations above a certain threshold (IC_{50} or IC_{90}) for sufficient pharmacological activity (54,55). At the same time, when drug-related toxicities can be linked to actual plasma concentrations, it is important to project the maximum concentrations achievable at the therapeutic dose (56,57). Multi-exponential PK in preclinical species can make projection of human PK more difficult and simple allometric scaling is generally not adequate. Therefore, alternative approaches (e.g., Dedrick plot, species-invariant time method, and Css-MRT method) are employed that afford projection of multi-exponential kinetics in man. The projection of absorption kinetics in humans, that is most certainly going to differ when the dosage form is altered from discovery into development, may also pose problems. As much as possible, therefore, attempts have been made at BMS to project absorption kinetics in humans by administering solid dosage forms (e.g., micronized suspension, unoptimized powder in capsule) to dogs and monkeys.

Projection of Human Efficacious Dose. As discussed, the success of the human efficacious dose projections was similar to that of the AUC projections. Compared to the data set used for human exposure projection, the data set for efficacious dose projections was smaller. Most of the compounds used in the exposure projections were either discontinued from development (prior to achieving clinical proof of concept) or there was insufficient clinical information available with respect to the likely efficacious dose. In some cases, the efficacious dose information was based on the biomarker data obtained in the clinic and as such, the accuracy of those projections was based on the relevance of the biomarker results as surrogate endpoints. Furthermore, projection of efficacious doses was heavily dependent on the animal disease models used in each of the therapeutic areas. Assumptions involved in projecting the efficacious dose go well beyond those used in the projection of human exposure. One not only needs to understand the PK/PD relationship associated with the drug action at the biological target, but one also needs to assume that the molecular basis of animal disease is similar to human disease, and that the drug molecules will act in a similar fashion in both species. Active metabolites further complicate efficacy projections, especially when their contribution varies from animal species to human (58,59).

Assessment of Projections. In the present prospective analysis, the success criteria were applied equally across all compounds in the data set and projections that fell within 4-fold of the observed value were considered "accurate" or "acceptable" (Table II). In reality, however, it is important to realize that the success criteria for individual molecules may differ. If the safety margin for a particular compound is narrow, a 3-fold error (e.g., under-projection) may lead to drug-related toxicities at the therapeutic dose. In addition, the dose level of the compound needs to be considered. For example, a projected dose of 1 mg (*versus* an actual dose of 3 mg) will likely not be problematic from a cost of goods or formulation standpoint. In contrast, so-called "high dose" compounds (≥200 mg) can be problematic and erroneous projections can lead to difficulties in the clinic. Of the ten compounds described (Table III), five were high dose compounds and projection ratios for three (BMS-34, BMS-25, and BMS-36) were >2. Fortunately, the dose of BMS-25 and BMS-36 at the time of their nomination was over-projected (70 *versus* 30 mg; and 150 *versus* 25 mg, respectively) and no formulation issues were encountered in the clinic. For BMS-34, the dose was under-projected (300 *versus* 400 to 1,000 mg) and formulation options were available at the time of dose escalation that enabled the attainment of an efficacious dose.

Multiple Approaches. When comparing the various projection methods, it is clear that no one method is more

successful than another. In fact, it is the combination of various methods yielding similar projections that gives one greater confidence at the time of compound nomination.

In this analysis, only average values of different parameters obtained from the *in vitro* and *in vivo* preclinical studies were used. No attempt was made to consider the uncertainties associated with each of the methods described. It is acknowledged that projections based on point estimates will more often than not represent a highly optimistic view of the suitability for further development of a drug candidate. In practice, it is desirable to incorporate known uncertainty into such projections. A formal representation of the uncertainty would allow one to understand the risks associated with the decision to advance the drug candidate in question and thus enable better decision making.

It is again important to emphasize that all the projections described herein were conducted prospectively. Therefore, the compiled data set truly reflects the reality that pharmaceutical companies face when making critical decisions at the time of compound nomination. To date, most of the literature has merely described retrospective analyses of successful projections. To further explore why certain projections are successful, a retrospective analysis will be conducted by applying all the methods described here to individual compounds in the current dataset. The accuracy of each approach will be assessed for a future report. In addition, it is anticipated that additional compounds will be added as more clinical data become available. Further analyses will focus also on the projection of peak-to-trough ratios in man (plasma C_{max}/C_{min} ratio) and the overall shape of the plasma concentration-time curve.

CONCLUSIONS AND FUTURE DIRECTION

Over a period of 8 years, it was possible to successfully project human AUC and efficacious dose for 90% of all BMS compounds prior to first-in-human studies. Because prospective projections are difficult, especially for the first-in-class compounds, the use of more than one method for consistency in projections is strongly recommended. It is obvious too that clinical data for lead compounds are extremely useful and that this highlights the importance of close communication between development and discovery scientists within the pharmaceutical industry.

In recent years there has been an explosion in knowledge related to drug transporters and their impact on drug disposition, tissue distribution, and PK. Going forward it is possible that one may be able to evaluate species differences and incorporate such information in human PK and dose projections (60,61). Similarly, the increased availability of computing power and software packages has enabled the development of PB/PK-based models (42,62,63). Such physiological models allow one to conduct extrapolations across species in a more mechanistic fashion. Disposition of the drug and PK profile can be simulated with knowledge of tissue size, tissue perfusion, drug permeability, binding of drug between the tissue and blood as well as elimination from certain tissues (64,65). Even transporter information can be incorporated into such models. Therefore, it is likely that human PK and dose projections will be conducted with an ever increasing array of tools and approaches. However, successful projections of human AUC, peak-to-trough, C_{max}, C_{min}, half-ife, clearance,and efficacy will always depend on the quality of the non-clinical data and its careful integration.

ACKNOWLEDGMENTS

The authors would like to thank all of the BMS colleagues who made the various data available for collation. Their help is greatly appreciated.

REFERENCES

1. I. Kolaand, and J. Landis. Can the pharmaceutical industry reduce attrition rates? *Nat. Rev. Drug Discov.* **3**:711–715 (2004).
2. G. W. Caldwell, J. A. Masucci, Z. Yan, and W. Hageman. Allometric scaling of pharmacokinetic parameters in drug discovery: can human CL, Vss and t1/2 be predicted from *in vivo* rat data? *Eur. J. Drug Metab. Pharmacokinet.* **29**:133–143 (2004).
3. K. Bachmann, J. Byers, and R. Ghosh. Prediction of *in vivo* hepatic clearance from *in vitro* data using cryopreserved human hepatocytes. *Xenobiotica*. **33**:475–483 (2003).
4. A. R. Hilgers, D. P. Smith, J. J. Biermacher, J. S. Day, J. L. Jensen, S. M. Sims, W. J. Adams, J. M. Friis, J. Palandra, J. D. Hosley, E. M. Shobe, and P. S. Burton. Predicting oral absorption of drugs: a case study with a novel class of antimicrobial agents. *Pharm. Res.* **20**:1149–1155 (2003).
5. R. S. Obach, J. G. Baxter, T. E. Liston, B. M. Silber, B. C. Jones, F. MacIntyre, D. J. Rance, and P. Wastall. The prediction of human pharmacokinetic parameters from preclinical and *in vitro* metabolism data. *J. Pharmacol. Exp. Ther.* **283**:46–58 (1997).
6. M. R. Shiran, N. J. Proctor, E. M. Howgate, K. Rowland-Yeo, G. T. Tucker, and A. Rostami-Hodjegan. Prediction of metabolic drug clearance in humans: *in vitro-in vivo* extrapolation *vs* allometric scaling. *Xenobiotica*. **36**:567–580 (2006).
7. G. J. Pass, D. Carrie, M. Boylan, S. Lorimore, E. Wright, B. Houston, C. J. Henderson, and C. R. Wolf. Role of hepatic cytochrome p450s in the pharmacokinetics and toxicity of cyclophosphamide: studies with the hepatic cytochrome p450 reductase null mouse. *Cancer Res.* **65**:4211–4217 (2005).
8. F. Van Bambeke, J. M. Michot, J. Van Eldere, and P. M. Tulkens. Quinolones in 2005: an update. *Clin. Microbiol. Infect.* **11**:256–280 (2005).
9. U. Theuretzbacher, F. Ihle, and H. Derendorf. Pharmacokinetic/pharmacodynamic profile of voriconazole. *Clin. Pharmacokinet.* **45**:649–663 (2006).
10. P. Gaussem, J.L. Reny, C. Thalamas, N. Chatelain, M. Kroumova, B. Jude, B. Boneu, and J.N. Fiessinger. The specific thromboxane receptor antagonist S18886: pharmacokinetic and pharmacodynamic studies. *J. Thromb. Haemost.* **3**:1437–1445 (2005).
11. I. Mahmoodand, and J. D. Balian. The pharmacokinetic principles behind scaling from preclinical results to phase I protocols. *Clin. Pharmacokinet.* **36**:1–11 (1999).
12. C. Ramachandran, P. K. Nair, A. Alamo, C. B. Cochrane, E. Escalon, and S. J. Melnick. Anticancer effects of amooranin in human colon carcinoma cell line *in vitro* and in nude mice xenografts. *Int. J. Cancer.* **119**:2443–2454 (2006).
13. S. Jones-Bolin, H. Zhao, K. Hunter, A. Klein-Szanto, and B. Ruggeri. The effects of the oral, pan-VEGF-R kinase inhibitor

CEP-7055 and chemotherapy in orthotopic models of glioblastoma and colon carcinoma in mice. *Mol. Cancer. Ther.* **5**:1744–1753 (2006).
14. H. Kai, K. Shibuya, Y. Wang, H. Kameta, T. Kameyama, S. Tahara-Hanaoka, A. Miyamoto, S. Honda, I. Matsumoto, A. Koyama, T. Sumida, and A. Shibuya. Critical role of M. tuberculosis for dendritic cell maturation to induce collagen-induced arthritis in H-2b background of C57BL/6 mice. *Immunology*. **118**:233–239 (2006).
15. V. L. Kumar, S. Roy, R. Sehgal, and B. M. Padhy. A comparative study on the efficacy of rofecoxib in monoarticular arthritis induced by latex of Calotropis procera and Freund's complete adjuvant. *Inflammopharmacology*. **14**:17–21 (2006).
16. C. M. Paulos, B. Varghese, W. R. Widmer, G. J. Breur, E. Vlashi, and P. S. Low. Folate-targeted immunotherapy effectively treats established adjuvant and collagen-induced arthritis. *Arthritis Res. Ther.* **8**:R77 (2006).
17. C. M. Lee, and L. Farde. Using positron emission tomography to facilitate CNS drug development. *Trends Pharmacol. Sci.* **27**:310–316 (2006).
18. R. T. Lewis, W. P. Blackaby, T. Blackburn, A. S. Jennings, A. Pike, R. A. Wilson, D. J. Hallett, S. M. Cook, P. Ferris, G. R. Marshall, D. S. Reynolds, W. F. Sheppard, A. J. Smith, B. Sohal, J. Stanley, S. J. Tye, K. A. Wafford, and J.R. Atack. A pyridazine series of alpha2/alpha3 subtype selective GABA A agonists for the treatment of anxiety. *J. Med. Chem.* **49**:2600–2610 (2006).
19. S. Heck, X. Qian, and M. Velleca. Genetically engineered mouse models for drug discovery: new chemical genetic approaches. *Curr. Drug Discov. Technol.* **1**:13–26 (2004).
20. J. Tornell, and M. Snaith. Transgenic systems in drug discovery: from target identification to humanized mice. *Drug Discov. Today.* **7**:461–470 (2002).
21. S. L. Hu. Non-human primate models for AIDS vaccine research. *Curr. Drug Targets Infect. Disord.* **5**:193–201 (2005).
22. N. L. Haigwood. Predictive value of primate models for AIDS. *AIDS Rev.* **6**:187–198 (2004).
23. N. M. Kneteman, A. J. Weiner, J. O'Connell, M. Collett, T. Gao, L. Aukerman, R. Kovelsky, Z. J. Ni, Q. Zhu, A. Hashash, J. Kline, B. Hsi, D. Schiller, D. Douglas, D. L. Tyrrell, and D. F. Mercer. Anti-HCV therapies in chimeric scid-Alb/uPA mice parallel outcomes in human clinical application. *Hepatology*. **43**:1346–1353 (2006).
24. R. L. Dedrick. Animal scale-up. *J. Pharmacokinet. Biopharm.* **1**:435–461 (1973).
25. J. B. Houston. Utility of *in vitro* drug metabolism data in predicting *in vivo* metabolic clearance. *Biochem. Pharmacol.* **47**:1469–1479 (1994).
26. B. A. Hoener. Predicting the hepatic clearance of xenobiotics in humans from *in vitro* data. *Biopharm. Drug Dispos.* **15**:295–304 (1994).
27. T. Iwatsubo, N. Hirota, T. Ooie, H. Suzuki, and Y. Sugiyama. Prediction of *in vivo* drug disposition from *in vitro* data based on physiological pharmacokinetics. *Biopharm. Drug Dispos.* **17**:273–310 (1996).
28. R. S. Obach. Nonspecific binding to microsomes: impact on scale-up of *in vitro* intrinsic clearance to hepatic clearance as assessed through examination of warfarin, imipramine, and propranolol. *Drug Metab. Dispos.* **25**:1359–1369 (1997).
29. B. Davies, and T. Morris. Physiological parameters in laboratory animals and humans. *Pharm. Res.* **10**:1093–1095 (1993).
30. D. E. Wildman. A map of the common chimpanzee genome. *Bioessays.* **24**:490–493 (2002).
31. W. F. Mueller, F. Coulston, and F. Korte. The role of the chimpanzee in the evaluation of the risk of foreign chemicals to man. *Regul. Toxicol. Pharmacol.* **5**:182–189 (1985).
32. B. M. Nath, K. E. Schumann, and J. D. Boyer. The chimpanzee and other non-human-primate models in HIV-1 vaccine research. *Trends Microbiol.* **8**:426–431 (2000).
33. H. Wong, S. J. Grossman, S. A. Bai, S. Diamond, M. R. Wright, J. E. Grace, Jr., M. Qian, K. He, K. Yeleswaram, and D. D. Christ. The chimpanzee (Pan troglodytes) as a pharmacokinetic model for selection of drug candidates: model characterization and application. *Drug Metab. Dispos.* **32**:1359–1369 (2004).
34. H. Boxenbaum, and R. Ronfeld. Interspecies pharmacokinetic scaling and the Dedrick plots. *Am. J. Physiol.* **245**:R768–R775 (1983).
35. I. Mahmood, and R. Yuan. A comparative study of allometric scaling with plasma concentrations predicted by species-invariant time methods. *Biopharm. Drug Dispos.* **20**:137–144 (1999).
36. T. Wajima, Y. Yano, K. Fukumura, and T. Oguma. Prediction of human pharmacokinetic profile in animal scale up based on normalizing time course profiles. *J. Pharm. Sci.* **93**:1890–1900 (2004).
37. D. M. Jonker, L. A. Kenna, D. Leishman, R. Wallis, P. A. Milligan, and E. N. Jonsson. A pharmacokinetic–pharmacodynamic model for the quantitative prediction of dofetilide clinical QT prolongation from human ether-a-go-go-related gene current inhibition data. *Clin. Pharmacol. Ther.* **77**:572–582 (2005).
38. K. A. Walters, M. A. Joyce, J. C. Thompson, M. W. Smith, M. M. Yeh, S. Proll, L. F. Zhu, T. J. Gao, N. M. Kneteman, D. L. Tyrrell, and M. G. Katze. Host-specific response to HCV infection in the chimeric SCID-beige/Alb-uPA mouse model: role of the innate antiviral immune response. *PLoS Pathog.* **2**:0591–0602 (2006).
39. P. Turrini, R. Sasso, S. Germoni, I. Marcucci, A. Celluci, Di A. Marco, E. Marra, G. Paonessa, A. Eutropi, R. Laufer, G. Migliaccio, and J. Padron. Development of humanized mice for the study of hepatitis C virus infection. *Transplant Proc.* **38**:1181–1184 (2006).
40. M. van der Lee, G. Verweel, R. de Groot, and D. Burger. Pharmacokinetics of a once-daily regimen of lopinavir/ritonavir in HIV-1-infected children. *Antivir. Ther.* **11**:439–445 (2006).
41. P. Yeni. Tipranavir: a protease inhibitor from a new class with distinct antiviral activity. *J. Acquir. Immune. Defic. Syndr.* **34**:S91–S94 (2003).
42. H. M. Jones, N. Parrott, K. Jorga, and T. Lave. A novel strategy for physiologically based predictions of human pharmacokinetics. *Clin. Pharmacokinet.* **45**:511–542 (2006).
43. CDER. Guidance for industry: estimating the maximum safe starting dose in initial clinical trials for therapeutics in adult healthy volunteers. Available at: http://www.fda.gov/cder/guidance/5541fnl.htm, (2005).
44. K. W. Ward, R. Nagilla, and L. J. Jolivette. Comparative evaluation of oral systemic exposure of 56 xenobiotics in rat, dog, monkey and human. *Xenobiotica*. **35**:191–210 (2005).
45. J. F. Levesque, M. Gaudreault, R. Houle, and N. Chauret. Evaluation of human hepatocyte incubation as a new tool for metabolism study of androstenedione and norandrostenedione in a doping control perspective. *J. Chromatogr. B Analyt. Technol. Biomed. Life Sci.* **780**:145–153 (2002).
46. Q. Wang, R. Jia, C. Ye, M. Garcia, J. Li, and I. J. Hidalgo. Glucuronidation and sulfation of 7-hydroxycoumarin in liver matrices from human, dog, monkey, rat, and mouse. *In Vitro Cell Dev. Biol. Anim.* **41**:97–103 (2005).
47. I. Mahmood, and J. D. Balian. Interspecies scaling: predicting clearance of drugs in humans. Three different approaches. *Xenobiotica*. **26**:887–895 (1996).
48. T. Lave, A. H. Schmitt-Hoffmann, P. Coassolo, B. Valles, G. Ubeaud, B. Ba, R. Brandt, and R. C. Chou. A new extrapolation method from animals to man: application to a metabolized compound, mofarotene. *Life Sci.* **56**:PL473–PL478 (1995).
49. R. Nagilla, and K. W. Ward. A comprehensive analysis of the role of correction factors in the allometric predictivity of clearance from rat, dog, and monkey to humans. *J. Pharm. Sci.* **93**:2522–2534 (2004).
50. D. Sun, L. X. Yu, M. A. Hussain, D. A. Wall, R. L. Smith, and G. L. Amidon. *In vitro* testing of drug absorption for drug 'developability' assessment: forming an interface between *in vitro* preclinical data and clinical outcome. *Curr. Opin. Drug Discov. Devel.* **7**:75–85 (2004).
51. E. S. Kostewicz, M. Wunderlich, U. Brauns, R. Becker, T. Bock, and J. B. Dressman. Predicting the precipitation of poorly

soluble weak bases upon entry in the small intestine. *J. Pharm. Pharmacol.* **56**:43–51 (2004).
52. J. B. Dressman, and C. Reppas. *In vitro–in vivo* correlations for lipophilic, poorly water-soluble drugs. *Eur. J. Pharm. Sci.* **11**:S73–S80 (2000).
53. H. Wei, and R. Lobenberg. Biorelevant dissolution media as a predictive tool for glyburide a class II drug. *Eur. J. Pharm. Sci.* **29**:45–52 (2006).
54. Y. Gan, M. G. Wientjes, R. A. Badalament, and J. L. Au. Pharmacodynamics of doxorubicin in human bladder tumors. *Clin. Cancer Res.* **2**:1275–1283 (1996).
55. D. B. Mendel, A. D. Laird, X. Xin, S. G. Louie, J. G. Christensen, G. Li, R. E. Schreck, T. J. Abrams, T. J. Ngai, L. B. Lee, L. J. Murray, J. Carver, E. Chan, K. G. Moss, J. O. Haznedar, J. Sukbuntherng, R. A. Blake, L. Sun, C. Tang, T. Miller, S. Shirazian, G. McMahon, and J. M. Cherrington. In vivo antitumor activity of SU11248, a novel tyrosine kinase inhibitor targeting vascular endothelial growth factor and platelet-derived growth factor receptors: determination of a pharmacokinetic/pharmacodynamic relationship. *Clin. Cancer Res.* **9**:327–337 (2003).
56. N. Masuda, K. Matsui, N. Yamamoto, T. Nogami, K. Nakagawa, S. Negoro, K. Takeda, N. Takifuji, M. Yamada, S. Kudoh, T. Okuda, S. Nemoto, K. Ogawa, H. Myobudani, S. Nihira, and M. Fukuoka. Phase I trial of oral 2′-deoxy-2′-methylidenecytidine: on a daily×14-day schedule. *Clin. Cancer Res.* **6**:2288–2294 (2000).
57. C. Sessa, M. Zucchetti, M. Ghielmini, J. Bauer, M. D'Incalci, J. de Jong, H. Naegele, S. Rossi, M. A. Pacciarini, L. Domenigoni, and F. Cavalli. Phase I clinical and pharmacological study of oral methoxymorpholinyl doxorubicin (PNU 152243). *Cancer Chemother. Pharmacol.* **44**:403–410 (1999).
58. A. Fura. Role of pharmacologically active metabolites in drug discovery and development. *Drug Discov. Today*. **11**:133–142 (2006).
59. A. Fura, Y. Z. Shu, M. Zhu, R. L. Hanson, V. Roongta, and W. G. Humphreys. Discovering drugs through biological transformation: role of pharmacologically active metabolites in drug discovery. *J. Med. Chem.* **47**:4339–4351 (2004).
60. K. Bleasby, J. C. Castle, C. J. Roberts, C. Cheng, W. J. Bailey, J. F. Sina, A. V. Kulkarni, M. J. Hafey, R. Evers, J. M. Johnson, R. G. Ulrich, and J. G. Slatter. Expression profiles of 50 xenobiotic transporter genes in humans and pre-clinical species: a resource for investigations into drug disposition. *Xenobiotica*. **36**:963–988 (2006).
61. Y. Shitara, T. Horie, and Y. Sugiyama. Transporters as a determinant of drug clearance and tissue distribution. *Eur. J. Pharm. Sci.* **27**:425–446 (2006).
62. F. P. Theil, T. W. Guentert, S. Haddad, and P. Poulin. Utility of physiologically based pharmacokinetic models to drug development and rational drug discovery candidate selection. *Toxicol. Lett.* **138**:29–49 (2003).
63. S. J. Franks, M. K. Spendiff, J. Cocker, and G. D. Loizou. Physiologically based pharmacokinetic modelling of human exposure to 2-butoxyethanol. *Toxicol. Lett.* **162**:164–173 (2006).
64. S. Bjorkman, D. R. Wada, B. M. Berling, and G. Benoni. Prediction of the disposition of midazolam in surgical patients by a physiologically based pharmacokinetic model. *J. Pharm. Sci.* **90**:1226–1241 (2001).
65. S. Bjorkman. Prediction of drug disposition in infants and children by means of physiologically based pharmacokinetic (PBPK) modelling: theophylline and midazolam as model drugs. *Br. J. Clin. Pharmacol.* **59**:691–704 (2005).